International Journal of Recent Innovations in Academic Research
E-ISSN: 2635-3040; P-ISSN: 2659-1561
Homepage: https://www.ijriar.com/
Volume-8, Issue-12, December-2024: 1-13

Research Article

Biodiesel Production from Neem Seed Oil Using Nanocatalyst Prepared from Cow Horn via Response Surface Methodology (RSM) Optimization

***[a&b]Jude Edogbo Eneche, [a]Iliya Ibrahim Nkafamiya, [c]Kefas Wathagrda Shalbugau and [a]Joshua Gidigbi Ayodeji**

[a]Department of Chemistry, Modibbo Adama University, Yola, Nigeria
[b]Department of Science Laboratory Technology, Federal Polytechnic Ohodo, Nigeria
[c]Department of Chemistry, University of Maiduguri, Borno State, Nigeria
*Corresponding Author Email: edogboeneche@gmail.com

Received: November 18, 2024 **Accepted:** December 08, 2024 **Published:** December 16, 2024

Abstract
Biodiesel is a promising global business with large and rapid expansion. Several experiments have been conducted to create biodiesel using heterogeneous catalysts such as CaO, with the goal of establishing a commercially viable and sustainable biodiesel business. This study focuses on collecting calcium oxide from cow horn and using it in the transesterification reaction to produce biodiesel from neem seed oil (NSO). Various operational elements were investigated for their respective impact on biodiesel output, and after optimizing the reaction parameters; a conversion rate of 94% was attained while retaining a reaction period of 4 hours, a methanol-to-oil molar ratio of 0.08, and a catalyst concentration of 1 wt%. Response surface methodology (RSM) models were used to refine and optimize these reaction parameters in order to get the highest possible biodiesel yield. As a result, RSM was able to achieve significantly greater yields (94%). This study shows great promise for large-scale commercial biodiesel production.
Keywords: Biodiesel, Cow Horn, Nano Catalyst, Waste Management, Response Surface Methodology, Neem Seed Oil.

1. Introduction
Energy is part of life's necessity as it fuels the accomplishment of any human endeavor. According to Obidike *et al.,* (2022), the demand for energy is increasing as its usage is expected to increase by 34% by 2035. Gidigbi and Abubakar (2023) affirmed that majority of energy generated are associated with fossil fuel processing which has placed huge demand on its processing. Unfortunately, fossil fuel is not sustainable and its processing pollutes the environment. Maulidiyah *et al.,* (2022) reported that fossil fuels release harmful substances such as carbon dioxide (CO_2), sulphur oxides such as SO_2, and SO_3, and hydrocarbon volatile solvents (HCs). Hence a need for more eco-friendly and sustainable fuel with less pollution effects. Biodiesel is a liquid fuel produced from vegetable oils or animal fats and alcohol that can be used in diesel engines either alone or in combination with diesel oil. According to Puagsang *et al.,* (2021) and Abdul-Wahab and Takase, (2019), biodiesel is an alternative biodegradable fuel generated from renewable resources such as vegetable oils, animal fats, and waste/spent oil. Aside from being environmentally friendly, Atabani *et al.,* (2012) reported that biodiesel is sustainable and biodegradable, has improved engine efficiency (Puagsang *et al.,* 2021), and is simple to produce (Datta and Mandal, 2016). According to research, the yield and quality of biodiesel produced during the transesterification process are influenced by processing parameters. Several studies, including Abdul-Wahab and Takase (2019), have demonstrated that optimizing processing parameters such as temperature, time, catalyst loading, and methanol: oil ratios. The results showed that the RSM model performed better at predicting biodiesel output. As a result, the focus of the present study is to optimize the production and surface resonance morphology of biodiesel made from neem seed oil using a developed aluminum cow horn nano catalyst (AL-CHNC).

2. Materials and Methods
2.1. Materials
Methanol (99.5 % purity), sulphuric acid (98% BDH), aluminum nitrate, distilled water, crucibles, electric digital precision weighing balance (Ohaus, Adventurer, Model AR 3130), muffle furnace, heating mantle and

magnetic stirrer, rotary evaporator, thermometer, beakers, separating funnel, sample bottles, 150μm sieve, conical flask.

2.2. Methodology

2.2.1. Extraction and Esterification of Neem Seed Oil

Neem seed used were gotten from the neem trees at Modibbo Adama University, Yola. The neem seeds were sun dried for 7 days. The neem seed oil was extracted from the neem seeds using soxhlet extraction method. Esterification reaction (reduction of free fatty acid) was carried out using sulphuric acid (H_2SO_4) according to the method described by Gidigbi and Abubakar (2023). The neem seed oil was heated first at 60^{o}C for 20 mins to remove residue moisture. Then, 60ml of methanol was introduced into a 500ml conical flask containing 200ml of preheated neem seed oil and 0.3ml of H_2SO_4 was subsequently introduced. The mixture was placed on a hot plate with magnetic stirrer for 60 minutes at 50^{o}C. The mixture was separated by separating funnel with glycerine at lower layer, and esterified oil at upper layer and percentage yield was determined using the equation.

$$\% \text{ Oil yield} = \frac{\text{Weight of the oil (g)}}{\text{Weight of the dried sample (g)}} \text{ X } 100 \quad (1)$$

$$\% \text{ Oil yield} = \frac{20.5}{50} \text{ X } 100$$

$$\% \text{ Oil yield} = 41\%$$

2.2.2. Preparation of the Cow Horn and Aluminum Impregnated Cow Horn Nanocatalyst

The cow horn catalyst was prepared according to the method described by Amenaghawon *et al.,* (2021).

2.3. Characterisation of Biodiesel

2.3.1. Percentage (%) Yield

The percentage yield of the biodiesel was done according to the procedure described by Gidigbi and Abubakar (2023). The percentage biodiesel yield was calculated as follows:

$$\% \text{ Biodiesel yield} = \frac{\text{Weight of the biodiesel produced (g)}}{\text{Weight of the neems seed oil used (g)}} \text{ X } 100 \quad (2)$$

For the impregnated cow horn catalyst (Al-CHNC)

$$\% \text{ Biodiesel yield} = \frac{45.9\text{g}}{50\text{g}} \text{ X } 100$$

$$\% \text{ Biodiesel yield} = \frac{4590}{50} = 91.8\%$$

2.3.2. Determination of Specific Gravity

Specific gravity was determined according to ASTM D1298 method. A dry empty 50cm^3 density bottle was weighed and the mass was recorded as W_0, it was then fill with water and weighed again, the mass was recorded as W_1. The bottle was filled with the sample and it was weighed again, the mass was recorded as W_2. The specific gravity of all the samples were calculated using equation (1) (Al-Harbawy and Al-Mallah, 2014).

$$\text{Specific gravity} = \frac{W2 - WO}{W1 - W0} \quad (3)$$

2.3.3. Determination of Flash Point

The flash point is an ability of a sample to produce an inflammable mixture with an ignition source. 15 ml of the biodiesel pour into a 250 ml conical flask was heated and passed over the surface of the liquid. The temperature, at which the vapour ignited, was recorded as the flash point temperature. Three determinations were obtained. The sample was heated in a test cup at 1^{o}C per minute with a constant stirring. A small test flame was directed into the cup with simultaneous interruption. The flash point was taken as the temperature when the test flame causes the vapour above the sample to cause a distinct flash in the interior of the test cup (ASTM D93, 2020).

2.3.4. Tests for Cloud Point and Pour Points

The oil sample (5cm^3) was measured in 5cm^3 test tube and placed in a freezer. The sample was taken out of the freezer every 1 min to check any visible changes and the temperature was measured (ASTM D2500, 2008).

2.3.4.1. Observation for Cloud Point: 15 ml of the biodiesel was placed in refrigerator for 1 hour. The sample was observed and the temperature at which the cloud first formed was recorded (Edeh *et al.,* 2018).

2.3.4.2. Observation for Pour Point: The minimum temperature at which a fuel sample flow is regarded as pour point. Immediately the sample is removed from refrigerator, it was scrutinized at 5^{o}C for it to flow, the minimum temperature which the biodiesel flow was recorded as it pours point (Edeh *et al.,* 2018).

2.3.5. Determination of Kinematic Viscosity

The kinematic viscosity was determined according to ASTM D445 method. The viscometer was inserted into water bath at a set temperature of 40^{o}C and was left for 30 minutes. The sample was added into in the capillary tube of the viscometer and allowed to remain in the bath until it reached the test temperature of 100^{0}C. The sample was allowed to flow freely and the time required for the meniscus to pass from the first to the second timing mask was taken using stopwatch. Kinematic viscosity was calculated from viscometer calibration and measured flow time by using equation 4 (Indhumathi *et al.,* 2014).

$$V = C \times t \quad (4)$$

Where: V = Viscosity (cst), C = Viscosity tube constant and t = The afflux time in second

2.3.6. GC-MS of the Biodiesel

The biodiesel was assessed using Fourier transform infrared spectroscopy (FT-IR) and Gas chromatography-mass spectroscopy (GC-MS).

2.4. Experimental Design and RSM Modelling

A Box-Behnken design (BBD) was used to plan the transesterification experiments. The BBD was chosen for this study because it is suitable for modelling quadratic response surfaces. Four variables (Methanol-to-oil molar ratio, catalyst concentration, reaction time and temperature) known to influence biodiesel production were investigated. The ranges of these variables are shown in Table 1. Equation (5) is a quadratic regression model which was fitted to the experimental data generated from the 28 experimental runs produced by the BBD. The model terms were calculated via multiple regression analysis while analysis of variance (ANOVA) was used to assess the significance of the model terms. The experimental design and the accompanying statistical analysis were carried out using Design-Expert software version 13.0 (Stat-Ease Inc., Minneapolis, USA).

Table 1. Process parameters and their lower, middle and upper limits.

Variables	**Symbol**	**Coded and actual levels**		
		-1	**0**	**1**
Temperature (^{o}C)	A	55	62.5	70
Time (Hours)	B	2	3	4
Catalyst (wt%)	C	1	3	5
Methanol/oil ratio (Mol/mol)	D	0.08	0.215	0.35

The relationship of the process (independent) variables and the response is given by a second order polynomial as shown in equation (5).

$$Y_i = b_o + \sum biX_i + \sum b_{ij}X_iX_j + \sum b_{ii}X_i^{\,2} + e_i \quad (5)$$

Where,
Y_i denotes the predicted response,
b_o is the value at intercept,
b_i is the coefficient of first order,
b_{ii} is the quadratic effect coefficient,
b_{ij} is the interacting effect coefficient,
X_i and X_j are the process variables that affect the response, and

e_i is the experimental random error.

This resulted in generation of 28 experimental runs which were performed in the laboratory randomly, to avoid any systematic error in the outcomes.

3. Results and Discussion

3.1. FTIR Analysis of both the Neem Seed Oil and the Biodiesel

The Fourier transform infrared spectrometry (FTIR) was used to evaluate the possible functional groups present in biodiesel. It was an easy way to identify the presence of functional groups in the sample and its structure based on the energies associated with the molecular vibration when irradiated. Neem seed oil was run through FTIR, the bonds as well as functional groups present were found to respond differently to the incoming radiation, due to variation in their molecular vibration of stretching and bending. The response of the functional groups was characterized by observing the transmission of infrared radiations and comparing it with known standards in order to identify the type and the nature of functional groups present in the samples. The presence and the nature of functional groups among other factors provided information on the stability of the biodiesel fuel. The research was done to design and evaluate the functional groups and structure so as to establish the reactivity of the fuels as a function of possible degradation. The broad peak at 3484 cm^{-1} (neem oil) is due to O-H stretching vibrations in alcohols or carboxylic acids, typically found in neem oil. Its absence in the biodiesel spectrum (a) indicates a successful conversion of these functional groups into ester linkages (COO) during the transesterification process to produce biodiesel, this also correspond to the result reported by Gutiérrez-López *et al.,* (2021). The peaks at 2932 and 2867 cm^{-1} (neem oil) corresponds to C-H stretching vibrations in alkanes. The slight shift to lower wavenumbers in biodiesel (2929 and 2872 cm^{-1}) could be due to a change in chain conformation upon esterification. This is further supported by the shift in the carbonyl (C=O) stretching peak from 1749 cm^{-1} in neem oil to 1722 cm^{-1} in biodiesel. The shift to a lower wavenumber indicates a change in the bonding environment, likely due to the formation of ester carbonyl linkages (C=O) in biodiesel, compared to the triglycerides present in neem oil similar to the findings of Banik *et al.,* (2018). The peaks around 1461 and 1174 cm^{-1} (neem oil) are typically associated with C-H bending vibrations in alkanes. Their weakening suggests a potential decrease in alkane presence upon conversion to biodiesel.

The new peak at 1520 cm^{-1} in biodiesel is indicative of N-H bending vibrations, possibly arising from residual impurities or additives introduced during biodiesel production as reported by Khan (2021). The band located at 1097 cm^{-1} (O-CH_2-C) is visible in the neem seed oil spectrum but absent in the biodiesel spectrum suggesting the triglycerides conversion, the result is similar to the findings of Gutiérrez-López *et al.,* (2021). The FTIR analysis highlights the chemical changes that occur during neem oil conversion to biodiesel. The disappearance of the O-H peak and the shift in the C=O peak strongly suggest a successful transesterification process, converting carboxylic acids/alcohols in neem oil to biodiesel esters. The slight shifts in C-H stretching vibrations might be due to changes in the molecular conformation of the aliphatic chains. The weakening of some peaks in the biodiesel spectrum indicates a potential decrease in alkanes compared to neem oil. The new peak in biodiesel suggests the presence of nitrogen-containing compounds, which could be impurities or additives. Figure 1 shows the FTIR analysis of biodiesel and its precursor neem seed oil. It reveals a clear picture of the chemical transformation that occurs during the transesterification process.

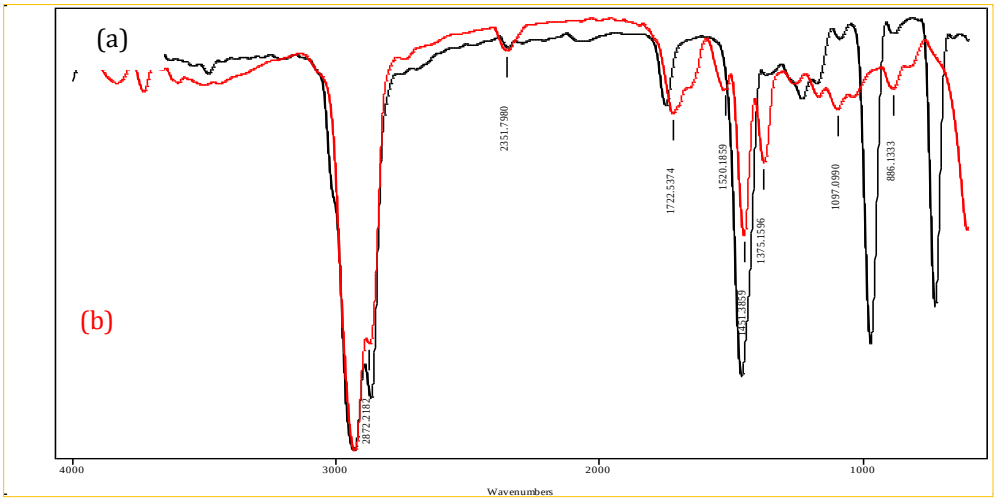

Figure 1. FTIR of (a) Biodiesel and (b) Neem oil.

3.2. Physiochemical Properties of Biodiesel

Table 2. Physicochemical characteristics of neem oil.

Parameter	Value
Percentage yield (%)	41.0
Colour	Pale green
Density	0.89
FFA	7.6
Flash point (°C)	183.1
Viscosity	4.6
Acid value (mgKOH/g)	15.06
Cloud point (°C)	15
Pour point (°C)	8

Table 3. Neem biodiesel properties and the acceptable range according to ASTM.

Property	Neem biodiesel	ASTM D6751 range for biodiesel
Acid value (mg of KOH/g)	0.27	<0.50
Free fatty acid (mg of KOH/g)	0.135	<0.50
Cloud point (˚C)	12	-3–15
Pour point (˚C)	8	-5–10
Flash point (˚C)	144.5	100–170
Energy content (MJ)	41.30	-
Specific gravity @15.5°C	0.88	0.88
Density, lb/gal @15.5°C	7.2	7.3
Kinematic viscosity (mm^2/s) @40˚C	4.31	4.0–6.0

The maximum yield of oil from the soxhlet extraction is 41.0%. The oil yield is higher when compared to 31.9% reported for neem seed oil by Barbosa *et al.,* (2023), while Ochi *et al.,* (2020) reported maximum yield of 38.50%, also 29.49% (Mustapha *et al.,* 2020). The high percentage oil yield is an indication of possible industrial application. Also, the operation condition such as types and volume of solvent, reaction temperature, reaction time and particle size are also influencing the yield of the oil as reported by Ochi *et al.,* (2020). The high non-polarity index of n-hexane, which aided its molecules to penetrate faster through the neem seeds paste was observed to aid the high yield in the n-hexane extraction method, this is consistent with the findings of Yang *et al.,* (2014).

The density of the extracted neem oil in this study is 0.89 g/cm^3 which is slightly higher compared to the density obtained 0.88 g/cm^3 using n-hexane as reported by Barbosa *et al.,* (2023). Also, the value of density from this study is lower compared with density of neem (0.95) obtained using petroleum ether and (0.99) using ethyl acetate as reported by Asseafa *et al.,* (2021). The acid value in this study (15.06) is similar to the acid value of neem seed oil (15.02) obtained by Ochi *et al.,* (2020) and higher when compared with acid value reported for n-hexane extraction of neem seed oil which is (6.73 and 7.93) for equal mixture of hexane and methanol as reported by Barbosa *et al.,* (2023), while slightly higher than the acid value (14.62) as reported by Hussein *et al.,* (2021). The acid value gives an indication of the amount of FFA present in the oil at the time of the test. The FFA of neem seed oil (7.6) in this study is slightly higher compare to FFA of neem (7.51) reported by Ochi *et al.,* (2020) and 3.38 as reported by Barbosa *et al.,* (2023).

Nevertheless, the low value of free fatty acids indicates low levels of hydrolytic and lipolytic activities in the oils. The flash point of neem seed oil in this study (183.1˚C) is slightly higher compare to (173˚C) reported by Mustapha *et al.,* (2020) and (167.80˚C) reported by Ochi *et al.,* (2020) for neem seed oil respectively. The flash point is an indicative of lowest temperature in which oil can ignite. The high flash point of neem seed oil is an indicative of its stability to combustion which is an important parameter to industrial application of any seed oil. The cloud point (15˚C) in this study is lower compared to cloud point value at (16˚C) as reported by Ochi *et al.,* (2020). The cloud point suggests the temperature at which the oil will form a wax. The low cloud point of neem seed oil is an indicative of its operability as a fuel. Pour point shows the lowest temperature at which oil flows in a specified laboratory test. It determines at which temperature a fuel remains fluid and can be pumped and used effectively. The pour point (8˚C) in this study is lower compared to the pour point (12˚C) obtained in neem seed oil as reported by Ochi *et al.,* (2020). This shows that neem seed oil can function as a fuel in Nigeria, even in the dry season.

3.3. GC-MS Analysis of both the Neem Seed Oil and Biodiesel

The neem oil and biodiesel produced from neem seed oil exhibit distinct chemical profiles, with both having unique major constituents. Neem oil's most abundant compounds are 9,17-Octadecadienal, (Z)- and 3,4-Octadiene, 7-methyl-, which make up 21.85% and 14.73% of its composition, respectively as presented in table 4. These compounds contribute to the oil's characteristic properties and potential applications. For instance, 9,17-Octadecadienal is a long-chain unsaturated aldehyde, which may impart specific oxidative stability and reactivity to neem oil. In contrast, 3,4-Octadiene, 7-methyl- is a smaller unsaturated hydrocarbon that could affect the oil's volatility and scent profile. The neem biodiesel, on the other hand as presented in table 5, is characterized by the presence of long-chain alkanes and branched alkanes. The most notable constituents include Hexadecane (5.82%), Hexadecane, 2,6,11,15-tetramethyl- (6.48%), and Decahydro-4,4,8,9,10-pentamethylnaphthalene (6.28%). These compounds suggest that neem biodiesel has a high content of saturated hydrocarbons, which are generally known for providing good combustion properties and higher cetane numbers. This composition is indicative of the biodiesel's potential efficiency and performance as a fuel, with likely improved ignition quality compared to unsaturated counterparts as reported by Ibrahim *et al.,* (2021).

When comparing the two, it is evident that neem oil contains a higher percentage of unsaturated compounds, which could make it more prone to oxidation and polymerization. These properties might be beneficial in specific contexts such as bioactive or medicinal applications where reactivity is desirable. On the contrary, the saturated nature of neem biodiesel's constituents suggests enhanced stability and better performance in combustion engines, making it a more suitable candidate for fuel applications (Madai *et al.,* 2020).

Neem oil's composition, dominated by unsaturated aldehydes and hydrocarbons, lends itself to uses where reactivity and bioactivity are beneficial. Neem biodiesel's saturated and branched alkanes make it a stable and efficient fuel source (Noreen *et al.,* 2021). Understanding these compositional differences is crucial for optimizing the use of each product in their respective applications, ensuring that their unique properties are fully leveraged.

Table 4. GC-MS analytical report of neem oil.

Chemical constituent	Molar mass (g/mol)	Chemical formula	Retention time (min)	Area percent
9,17-Octadecadienal, (Z)-	266.450	$C_{18}H_{34}O$	11.867	21.850
3,4-Octadiene, 7-methyl-	110.190	C_9H_{14}	16.492	14.730
cis-13-Octadecenoic acid, methyl ester	296.490	$C_{19}H_{36}O_2$	10.176	6.790
Hexadecanoic acid, methyl ester	270.450	$C_{17}H_{34}O_2$	10.511	4.100
9-Octadecenal, (Z)-	266.450	$C_{18}H_{34}O$	11.112	5.570
12-Methyl-E,E-2,13-octadecadien-1-ol	268.470	$C_{19}H_{36}O$	11.292	3.880
Z-4-Nonadecen-1-ol acetate	322.540	$C_{21}H_{38}O_2$	17.136	5.160
Decahydro-4,4,8,9,10-pentamethylnaphthalene	202.350	$C_{15}H_{26}$	9.432	1.550
Heptadecane	240.470	$C_{17}H_{36}$	14.720	2.050

Table 5. GC-MS analytical report of neem biodiesel.

Chemical constituent	Molar mass (g/mol)	Chemical formula	Retention time (min)	Area percent
Hexadecane	226.440	$C_{16}H_{34}$	11.733	5.820
Hexadecane,2,6,11,15-tetramethyl-	296.590	$C_{20}H_{42}$	12.385	6.480
Decahydro-4,4,8,9,10-pentamethylnaphthalene	202.350	$C_{15}H_{26}$	9.816	6.280
Tetradecane	198.390	$C_{14}H_{30}$	9.141	2.040
Dodecane, 4,6-dimethyl-	184.360	$C_{14}H_{30}$	7.619	1.170
1-Tridecene	182.350	$C_{13}H_{26}$	7.996	1.320
Benzocycloheptatriene	118.180	C_9H_{10}	8.483	1.190

3.4. Process Parameters Optimization Using RSM

The Box-Behnken design (BBD) was used to determine the relationship between neem seed oil yield and the process parameters chosen for the yield optimization study. This design was chosen because of its ability to accurately determine important process parameters. Table 7 shows the experimental matrix of yield values corresponding to the design points, as well as the values of all three variables generated by the Design-Expert 13 software.

The statistical accuracy and suitability of the quadratic polynomial equation created by response surface methodology (RSM), as well as the involvement of key influencing parameters, were determined using the analysis of variance (ANOVA) approach. Table 8 displays the results, demonstrating that the model is highly significant.

Factor coding is coded.

Sum of squares is type III-partial.

The model F-value of 2.73 in table 8 implies the model is significant. There is only a 3.95% chance that an F-value this large could occur due to noise.

P-values less than 0.0500 indicate model terms are significant. In this case A is a significant model term. Values greater than 0.1000 indicate the model terms are not significant. If there are many insignificant model terms (not counting those required to support hierarchy), model reduction may improve your model. The lack of fit F-value of 1.25 as shown in table 8 implies that it is not significant relative to the pure error. There is a 42.06% chance that a lack of fit F-value this large could occur due to noise. Non-significant lack of fit is good-we want the model to fit.

Table 6. (R^2) correlation coefficient, (SD) standard deviation, (CV) coefficient of variation.

SD	6.10	Adjusted R^2	0.4726
Mean	79.71	Predicted R^2	-0.5195
CV %	7.65	Adequate precision	7.0702
R^2	0.7461	-	

Table 7. Box-Behnken arrangements and responses.

SD	Run	Factor 1	Factor 2	Factor 3	Factor 4	Biodiesel yield	
		A: Temperature	B: Time	C: % catalyst	D: Methanol-oil ratio	Predicted value	Actual value
		C	H	wt%	G	%	%
1	1	70.000	2.000	1.000	0.080	83.370	80.000
12	2	55.000	2.000	5.000	0.350	75.510	74.000
28	3	62.500	3.000	3.000	0.215	77.570	87.000
21	4	62.500	3.000	3.000	0.050	83.590	85.000
9	5	70.000	2.000	1.000	0.350	72.750	73.000
20	6	62.500	3.000	6.340	0.215	80.610	79.000
6	7	55.000	4.000	5.000	0.080	72.930	76.000
10	8	55.000	4.000	1.000	0.350	75.720	81.000
14	9	70.000	4.000	5.000	0.350	89.670	93.000
24	10	62.500	3.000	3.000	0.215	77.570	72.000
17	11	62.500	1.314	3.000	0.215	82.670	83.000
4	12	55.000	2.000	5.000	0.080	82.130	86.000
15	13	49.860	3.000	3.000	0.215	62.480	54.000
27	14	62.500	3.000	3.000	0.215	77.570	75.000
11	15	70.000	4.000	1.000	0.350	87.840	83.000
13	16	55.000	4.000	5.000	0.350	75.610	78.000
23	17	62.500	3.000	3.000	0.215	77.570	82.000
18	18	62.500	4.686	3.000	0.215	87.640	84.000
25	19	62.500	3.000	3.000	0.215	77.570	80.000
8	20	55.000	2.000	1.000	0.350	70.920	75.000
16	21	75.140	3.000	3.000	0.215	81.830	87.000
3	22	70.000	4.000	1.000	0.080	89.160	94.000
2	23	55.000	4.000	1.000	0.080	69.980	69.000
19	24	62.500	3.000	0.500	0.215	74.080	71.000
26	25	62.500	3.000	3.000	0.215	77.570	74.000
22	26	62.500	3.000	3.000	0.440	81.050	77.000
5	27	70.000	2.000	5.000	0.080	92.960	91.000
7	28	70.000	4.000	5.000	0.080	94.050	89.000

Table 8. ANOVA outcomes using design-expert 13 (BBD) software.

Source	Sum of squares	Df	Mean square	F-value	p-value	-
Model	1421.78	14	101.56	2.73	0.0395	Significant
A: Temperature	558.72	1	558.72	15.01	0.0019	-
B: Time	38.63	1	38.63	1.04	0.3269	-
C: % Catalyst	85.68	1	85.68	2.30	0.1532	-
D: Methanol-oil ratio	59.55	1	59.55	1.60	0.2281	-
AB	77.07	1	77.07	2.07	0.1738	-
AC	2.91	1	2.91	0.0781	0.7842	-
AD	38.52	1	38.52	1.03	0.3276	-
BC	16.04	1	16.04	0.4310	0.5230	-
BD	62.83	1	62.83	1.69	0.2165	-
CD	7.24	1	7.24	0.1944	0.6665	-
A^2	58.22	1	58.22	1.56	0.2331	-
B^2	113.80	1	113.80	3.06	0.1040	-
C^2	1.31	1	1.31	0.0351	0.8542	-
D^2	65.12	1	65.12	1.75	0.2088	-
Residual	483.93	13	37.23	-	-	-
Lack of fit	322.60	8	40.32	1.25	0.4206	Not significant
Pure error	161.33	5	32.27	-	-	-
Cor Total	1905.71	27	-	-	-	-

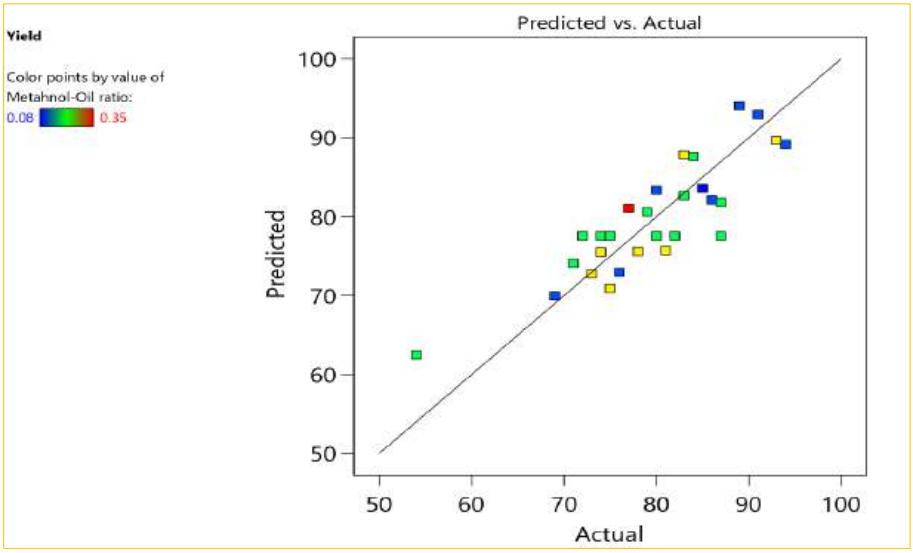

Figure 2. Predicted vs. actual FAME conversion.

Figure 2 demonstrates the correlation between the predicted data originated from the empirical model and the actual results attained through experiments. The correlation coefficient (R^2) and the adjusted-R^2 obtained were 0.7461 and 0.4726 respectively. The minor variance between R^2 and adjusted-R^2 denotes the significance and efficacy of all the reaction parameters involved.

3.5. Effect of Process Parameters to Optimize Biodiesel Production

The transesterification efficiency was examined by analyzing the combined effects of various process variables. Three-dimensional contour plots were implemented to visualize the interface between two independent parameters while maintaining the remaining variables at central levels. These contour plots helped establish the relationship among these parameters and establish the best levels for achieving maximum optimum yield.

In Figure 2a, the 3D surface plot illustrates the response surface curve depicting the relationship between reaction time and a constant temperature on biodiesel yield. Maintaining a methanol to oil ratio of 0.215 and a catalyst weight of 3wt%, at a reaction time of 3 hours caused an improved biodiesel yield of 87%. However, increasing the reaction time to 4.685 hours there was a decrease in biodiesel yield to 84%. Therefore,

biodiesel yield decreases with increase in reaction time this is similar to the findings reported by Oni-Adimabua, *et al.,* (2024). Furthermore at 49.86°C the yield was 54%, increasing the temperature to 62.5°C a biodiesel yield of 87% was observed and further increasing the temperature to 75°C, and lowering the reaction time to 3 hours a constant biodiesel yield of 87% was observed.

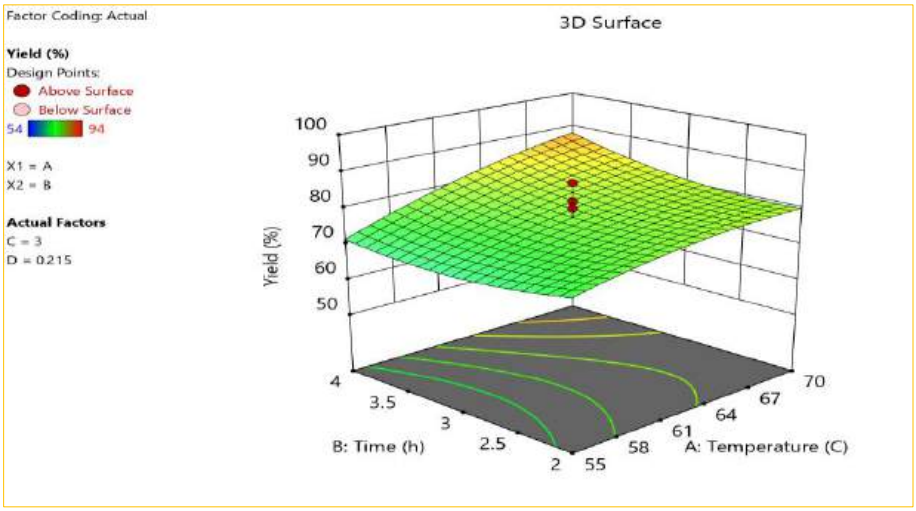

Figure 2a. Effect of reaction time and temperature on biodiesel yield.

The 3D surface in Figure 2b plot show correlation between catalyst loading and reaction temperature, and their collective influence on yield of biodiesel. Data indicates that a concurrent rise in both the temperature and the amount of catalyst leads to an enhancement in biodiesel production. At a temperature of 49.86°C the biodiesel yield is 54%. However, at 62.50°C an increase of 82% biodiesel yield was observed and at 75°C an increase in yield of 87% was observed this may be as a result of increase reaction activities as the temperature increases, the results is consistent with the findings reported by Ahmad *et al.,* (2023). Hence, it can be reasoned that the temperature of 70°C gave the best degree of conversion at optimum alcohol to oil molar ratio of 0.08 and 91% as seen in table 7.

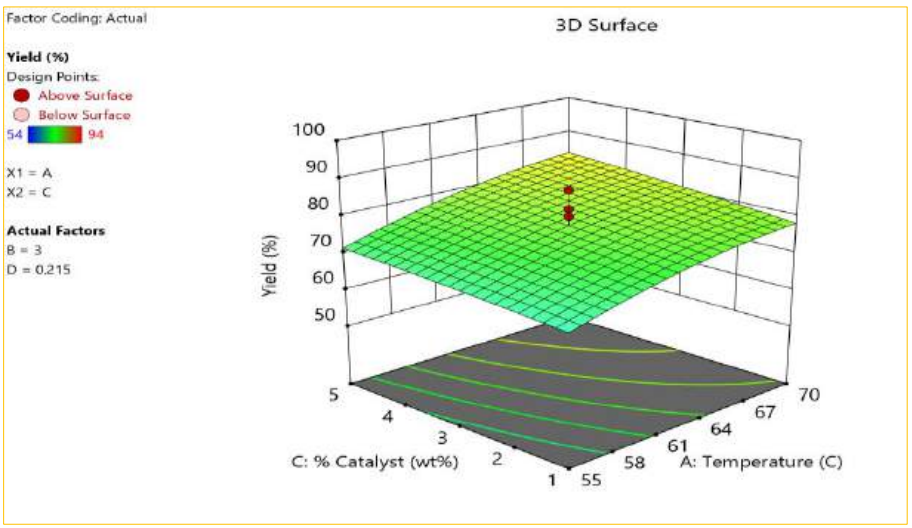

Figure 2b. Effect of catalysis loading and reaction temperature.

The effects of varying the methanol-to-oil ratio and the reaction temperature on the yield of biodiesel at a constant time of 3 hours and catalyst weight of 3wt% as illustrated in Figure 2c shows that a decrease in the molar ratio value of methanol-to-oil from 0.44 to a value of 0.05 showed an increase in biodiesel yield from 77.00% to 85% respectively. This, as a whole process, indicates that a higher methanol-to-oil ratio value acts as a considerable factor in enhancing the biodiesel production output as well as the temperature similar findings was reported by Oni-Adimabua, *et al.,* (2024).

The 3D surface in Figure 2d plot exhibits the effect of the catalyst concentration and the reaction time at 0.215 methanol to oil ratio and temperature of 62.50°C, at a catalyst concentration to 3wt% and keeping the

reaction duration at the mid-level value of 3 hours caused an improved biodiesel output of up to 82%. However, raising the catalyst concentration to 6.34wt% while maintaining the same reaction duration of 3 hours caused a decline in biodiesel yield to 79% the result is in agreement with the findings of Ahmad *et al.,* (2023).

The effects of varying the methanol-to-oil ratio and the reaction temperature on the yield of biodiesel, while maintaining a constant catalyst loading of 3wt% and temperature of 62.5^{o}C as shown in Figure 2e shows that a decrease in the molar ratio value of methanol-to-oil from 0.35 to a minimum value of 0.08 decreases the biodiesel yield from 93% to a minimum value of 54%. Selecting amid-point value of 0.215 for this factor and decreasing the transesterification reaction duration from 3 to 1.31 hours accelerates the transesterification rate, thus producing more biodiesel yield. This, as a whole process, indicates that a higher methanol-to-oil ratio value acts as a considerable factor in enhancing the biodiesel production output similar findings was reported by Ahmad *et al.,* (2023). The optimum value of the molar ratio of methanol-to-oil was estimated at 0.215. A further decrease in this molar ratio to less than 0.215 lowered the neem seed oil biodiesel output.

In Figure 2f, the influence of the methanol-to-oil ratio and catalyst quantity on production output of biodiesel is highlighted, considering fixed values of reaction temperature 62.5^{o}C and reaction duration 3 hours. Biodiesel output increases as the molar ratio of methanol-to-oil rises to 0.215. The maximum biodiesel output was observed at a catalyst quantity of 3wt%, reaching 87%. Nonetheless, the experimental matrix in Table 7 specifies that as the molar ratio value of methanol-to-oil stays unchanged at 0.215 and the catalyst amount is at its maximum value of 6.34 wt%, the biodiesel output is reduced to 79%. Therefore, catalyst concentration acts as a critical factor in enhancing biodiesel output similar to the findings reported by Oni-Adimabua *et al.,* (2024).

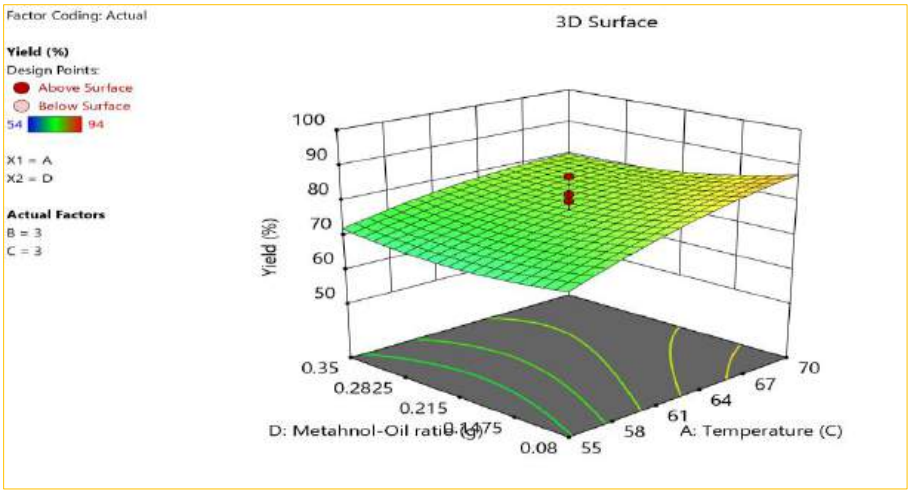

Figure 2c. Effect of methanol to oil and reaction temperature on the yield of biodiesel.

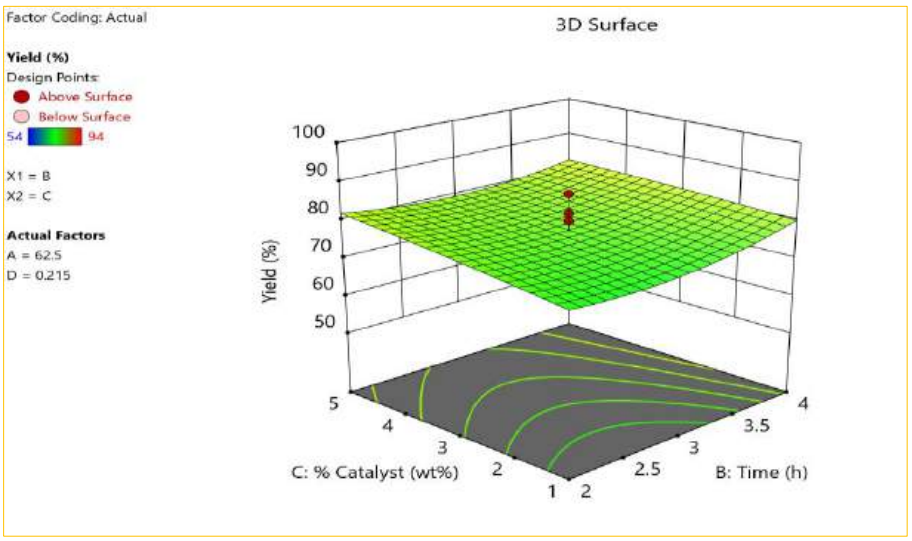

Figure 2d. Effect of catalyst concentration and the reaction time.

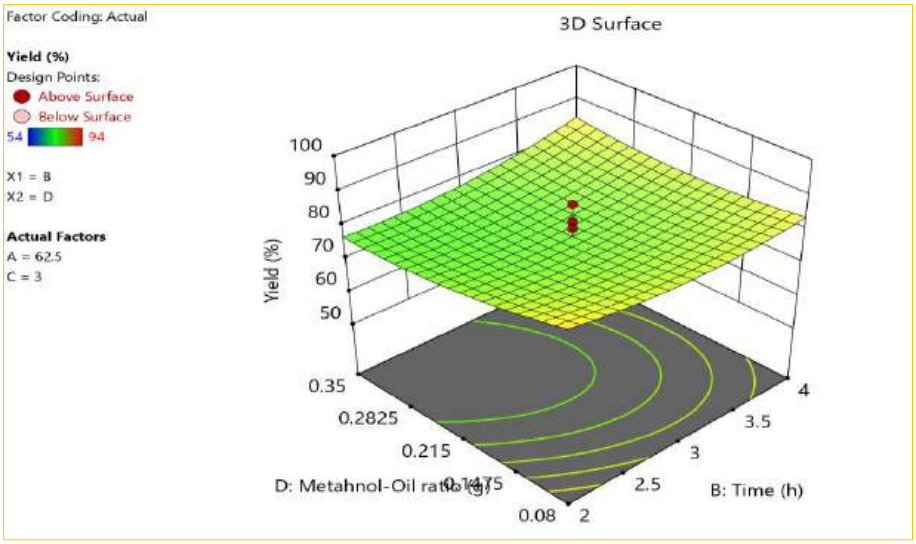

Figure 2e. Effect of methanol to oil ratio and reaction temperature.

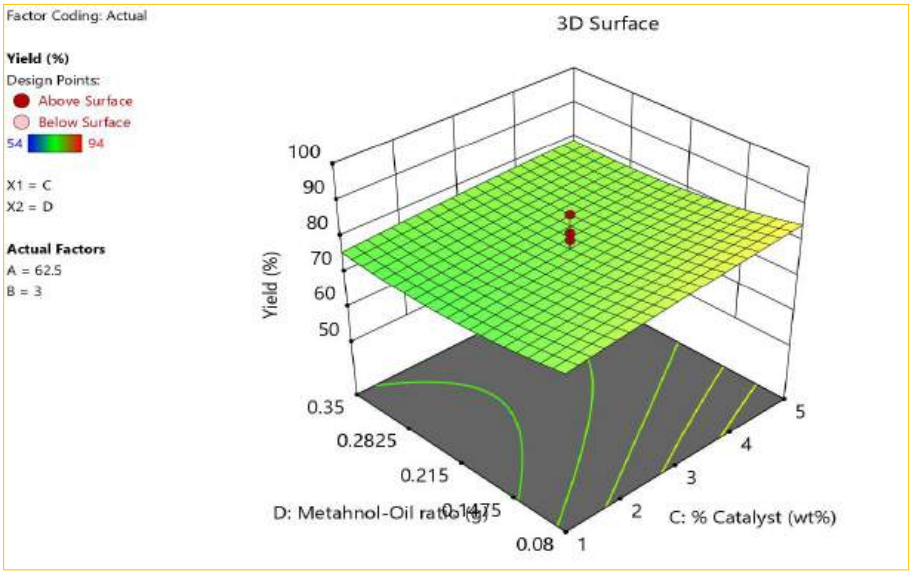

Figure 2f. Effect of methanol to oil ratio and catalyst loading.

4. Conclusions

In this work, a biodiesel generation and optimization study on neem seed oil was carried out using a cow horn CaO nanocatalyst via a transesterification reaction. The FAME content of neem seed oil biodiesel was determined using GCMS analysis. The fatty acid content, both saturated and unsaturated, was also determined by GC-MS analysis. The FFA value of neem seed oil was lowered from 7.6 mg KOH/g to 0.135 mg KOH/g following its conversion to biodiesel via transesterification. Using the RSM model, the biodiesel yield was optimized. The optimum biodiesel yield was recorded at process settings of 70^{o}C; 4 hours; 1wt% catalyst loading at 0.08 methanol: oil. The maximum anticipated biodiesel output was 94.05% using RSM, with a practical biodiesel yield attained experimentally of 94.00%. The applied RSM model forecasted biodiesel yield output with greater accuracy and computational speed. The RSM model showed modest errors of 0.003% when compared to the practical findings, showing that the models utilized in this investigation were highly accurate. The measured fuel properties of neem seed oil biodiesel were compared to and met the requirements of ASTM D6751.

Declarations

Acknowledgments: The authors would like to express their profound gratitude to Professor Iliya Nkafamiya, Professor Buba Ardo Aliyu of Chemistry Department, Modibbo Adama University Yola and Associate Professor Patrick Onoja of Chemical Engineering Department Modibbo Adama University Yola for their guidance during this research. Thanks are also due to all our colleagues for their help in various ways.

Author Contributions: JEE: Definition of intellectual content, implementation of study protocol, prepared first draft of manuscript, data collection, review manuscript and submission of article; IIN: Design of study,

statistical analysis and interpretation, literature survey, data collection, data analysis, manuscript preparation, editing, and manuscript revision; KWS: Concept, design, literature survey, manuscript revision; JGA: Manuscript revision, data analysis.

Conflict of Interest: The authors declare no conflict of interest.

Consent to Publish: The authors agree to publish the paper in International Journal of Recent Innovations in Academic Research.

Data Availability Statement: The data presented in this study are available on request from the corresponding author.

Funding: This research received no external funding.

Institutional Review Board Statement: Not applicable.

Informed Consent Statement: Not applicable.

Research Content: The research content of manuscript is original and has not been published elsewhere.

References

1. Abdul–Wahab, T. and Takase, M.A. 2019. Biodiesel production from neem (*Azadirachta indica*) seed oil. International Journal of Innovative Research and Development, 8(8): 33-40.
2. Ahmad, G., Imran, S., Farooq, M., Shah, A.N., Anwar, Z., Rehman, A.U. and Imran, M. 2023. Biodiesel production from waste cooking oil using extracted catalyst from plantain banana stem via RSM and ANN optimization for sustainable development. Sustainability, 15(18): 13599.
3. AL-Harbawy, A.W. and AL-Mallah, M.K. 2014. Production and characterization of biodiesel from seed oil of castor (*Ricinus communis* L.) plants. International Journal of Science and Technology, 3(9): 508-513.
4. Amenaghawon, A., Evbarunegbe, N.I. and Obahiagbon, K. 2021. Optimum biodiesel production from waste vegetable oil using functionalized cow horn catalyst: A comparative evaluation of some expert systems. Cleaner Engineering and Technology, 4: 100184.
5. Asseafa, H., Asteraye, Y. and Dagnaw, T. 2021. Biosciences and plant biology. International Journal of Current Research in Biosciences and Plant Biology, 8(1): 46-53.
6. ASTM D2500. 2008. Standard test method for cloud point and pour point of petroleum products. ASTM International.
7. ASTM D93. 2020. Standard test methods for flash point by Pensky-Martens closed cup tester. Available online at: https://www.astm.org/d0093-20.html
8. Atabani, A.E., Silitonga, A.S., Irfan, A.B., Mahlia, T.M.I., Masjuki, H.H. and Mekhilef, S. 2012. A comprehensive review on biodiesel as an alternative energy resource and its characteristics. Renewable and Sustainable Energy Review, 16(4): 2070- 2093.
9. Banik, S.K., Rouf, M.A., Rabeya, T., Khanam, M., Sajal, S.I., Sabur, S.B. and Islam, M.R. 2018. Production of biodiesel from neem seed oil. Bangladesh Journal of Scientific and Industrial Research, 53(3): 211-218.
10. Barbosa De Paulo, L.M., Oliveira Santos, J., Mouzinho de Sousa, R.C., Barros Furtado, J.L., Vidinha, P., Suller Garcia, M.A. and Fossatti Dall'Oglio, D. 2023. Bioherbicide from *Azadirachta indica* seed waste: Exploitation, efficient extraction of neem oil and allelopathic effect on *Senna occidentalis*. Recycling, 8(3): 50.
11. Datta, A. and Mandal, B. 2016. Comprehensive review of biodiesel as an alternative fuel for compression ignition engine. Renewable and Sustainable Energy Reviews, 57: 799-821.
12. Edeh, F., Joel, J.M., Yelwa, J.M. and Barminas, J.T. 2018. Development and characterization of heterogeneous kaolin/ash based catalyst system. Material Science: An Indian Journal, 16(3):141.
13. Gidigbi, J.A. and Abubakar, A.B. 2023. Optimisation of bio-diesel made from non-edible avocado seed oil (ASO) using homogenous H_2SO_4/KOH catalyst. International Journal of New Chemistry, 10(4): 242-257.
14. Gutiérrez-López, A.N., Mena-Cervantes, V.Y., García-Solares, S.M., Vazquez-Arenas, J. and Hernández-Altamirano, R. 2021. NaFeTiO4/Fe2O3–FeTiO3 as heterogeneous catalyst towards a cleaner and sustainable biodiesel production from *Jatropha curcas* L. oil. Journal of Cleaner Production, 304: 127106.
15. Hussein, J.B., Ilesanmi, J.O.Y., Yahuza, H.A. and Nkama, I. 2021. Effect of extraction methods and storage time on the yield and qualities of neem seed (*Azadirachta indica* A. Juss) oil. Nigerian Journal of Technological Development, 18(1): 55-62.

16. Ibrahim, I., Abdullahi, I. and Muhammad, F. 2021. Comparative analyses of biodiesel produced from neem and jatropha seed oil. Bayero Journal of Pure and Applied Sciences, 12(2): 141-143.

17. Indhumathi, P., Shabudeen Syed, P.S. and Shoba, U.S. 2014. A method for production and characterization of biodiesel from green micro algae. International Journal of Bio Science and Biotechnology, 6(5): 111-122.

18. Khan, T. 2021. Direct transesterification for biodiesel production and testing the engine for performance and emissions run on biodiesel-diesel-nano blends. Nanomaterials, 11(2): 417.

19. Madai, I.J., Chande Jande, Y.A. and Kivevele, T. 2020. Fast rate production of biodiesel from neem seed oil using a catalyst made from banana peel ash loaded with metal oxide (Li-CaO/Fe2 (SO4) 3). Advances in Materials Science and Engineering, 2020(1): 7825024.

20. Maulidiyah, M., Watoni, A.H., Maliana, N., Irwan, I. and Salim, L.A. 2022. Biodiesel production from crude palm oil using sulfuric acid and K2O catalysts through a two-stage reaction. Biointerface Research in Applied Chemistry, 12(3): 3150-3160.

21. Mustapha, A.O., Bawa, H.A. and Ali, K.S.M. 2020. Fuel properties of biodiesel from neem (*Azadirachta indica*) and jatropha (*Jatropha curcas*) seed oils using whole-cell biocatalyst. Journal of Chemical Society of Nigeria, 45(5): 925-934.

22. Noreen, S., Khalid, K., Iqbal, M., Baghdadi, H.B., Nisar, N., Siddiqua, U.H., Nisar, J., Noureddini, H. and Zhu, D. 1997. Kinetics of transesterification of soybean oil. Journal of the American Oil Chemists' Society, 74: 1457-1463.

23. Obidike, B.M., Okwara, N.O., Verlac, A.W., Enyoh, C. and Mbagwu, J.P. 2022. Optimization and effect of varying catalyst concentration and transesterification temperature on the yield of biodiesel production from palm kernel oil and groundnut oil. Analytical Methods in Environmental Chemistry Journal, 5(03): 55-69.

24. Ochi, D.O., Umeuzuegbu, J.C., Mahmud, H., Ekebafe, L.O. and Ani, M.O. 2020. Transesterification of neem (*Azadirachta indica*) seed oil. Nigerian Research Journal of Chemical Sciences, 8(1): 91-103.

25. Oni-Adimabua, O.N., Ifeanyi-Nze, F.O., Abimbolu, A.K., Opadokun, E.O., Omolusi, A.R., Ezeokolie, E.D. and Ankomah, N.O. 2024. Production, optimization, and characterization of biodiesel from almond seed oil using a bifunctional catalyst derived from waste animal bones and almond shell. European Journal of Sustainable Development Research, 8(3): em0261.

26. Puagsang, N., Chanakeawsomboon, I., Chantrapromma, S. and Palamanit, A. 2021. Production of biodiesel from low-grade crude palm oil using hydrochloric acid. EnvironmentAsia, 14(1): 23-32.

27. Yang, X., Lyu, H., Chen, K., Zhu, X., Zhang, S. and Chen, J. 2014. Selective extraction of bio-oil from hydrothermal liquefaction of *Salix psammophila* by organic solvents with different polarities through multistep extraction separation. BioResources, 9(3): 5219-5233.

Citation: Jude Edogbo Eneche, Iliya Ibrahim Nkafamiya, Kefas Wathagrda Shalbugau and Joshua Gidigbi Ayodeji. 2024. Biodiesel Production from Neem Seed Oil Using Nanocatalyst Prepared from Cow Horn via Response Surface Methodology (RSM) Optimization. International Journal of Recent Innovations in Academic Research, 8(12): 1-13.